

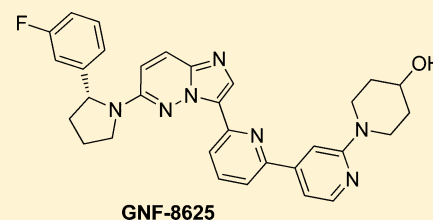
(R)-2-Phenylpyrrolidine Substituted Imidazopyridazines: A New Class of Potent and Selective Pan-TRK Inhibitors

Ha-Soon Choi, Paul V. Rucker, Zhicheng Wang, Yi Fan, Pamela Albaugh,[‡] Greg Chopiuk, Francois Gessier,[†] Fangxian Sun,[§] Francisco Adrian,[§] Guoxun Liu, Tami Hood,[⊥] Nanxin Li, Yong Jia, Jianwei Che,^{||} Susan McCormack, Allen Li, Jie Li, Auzon Steffy, AnneMarie Culazzo, Celine Tompkins, Van Phung, Andreas Kreuzsch, Min Lu, Bin Hu,[#] Apurva Chaudhary,[#] Mahavir Prashad,[#] Tove Tuntland, Bo Liu, Jennifer Harris, H. Martin Seidel,[⊥] Jon Loren, and Valentina Molteni*

Genomics Institute of the Novartis Research Foundation, 10675 John Jay Hopkins Drive, San Diego, California 92121, United States

Supporting Information

ABSTRACT: Deregulated kinase activities of tropomyosin receptor kinase (TRK) family members have been shown to be associated with tumorigenesis and poor prognosis in a variety of cancer types. In particular, several chromosomal rearrangements involving TRKA have been reported in colorectal, papillary thyroid, glioblastoma, melanoma, and lung tissue that are believed to be the key oncogenic driver in these tumors. By screening the Novartis compound collection, a novel imidazopyridazine TRK inhibitor was identified that served as a launching point for drug optimization. Structure guided drug design led to the identification of (R)-2-phenylpyrrolidine substituted imidazopyridazines as a series of potent, selective, orally bioavailable pan-TRK inhibitors achieving tumor regression in rats bearing KM12 xenografts. From this work the (R)-2-phenylpyrrolidine has emerged as an ideal moiety to incorporate in bicyclic TRK inhibitors by virtue of its shape complementarity to the hydrophobic pocket of TRKs.



KEYWORDS: Neurotrophins, tropomyosin receptor kinase, TRK, (R)-2-phenylpyrrolidine, imidazopyridazines, GNF-8625

The tropomyosin receptor kinase (TRK) receptors, TRKA, TRKB, and TRKC (also known as NTRK1, NTRK2 and NTRK3) and their respective neurotrophin ligands (NGF, BDNF, and NT-3) are implicated in proliferation, survival, differentiation, and functional regulation of different neuronal populations in the nervous system, especially during embryogenesis.¹ In the past decade, the dysregulation of neurotrophin signaling has been linked to the development and progression of cancer.^{2–9} Several different mechanisms have been proposed involving oncogenic activation of TRK receptors, expression of alternative and constitutively active splice variants under hypoxia conditions, point mutations, and genomic rearrangements.² TRKA rearrangement leading to constitutively active and ligand-independent fused protein TPM3-TRKA was originally identified in a colorectal carcinoma biopsy^{10,11} and was later found to be associated with a subset of papillary thyroid carcinomas (PTC).^{12–15} Recently the TPM3-TRKA fusion has also been described to be harbored in KM12 colorectal cells.¹⁶ Other TRKA fusions with TGF and TPR have been found in colorectal and thyroid cancers,^{10–15} and recently, TRKA fusions with MPRIP and CD74 have been identified in a subset of patients (3.3%) with lung adenocarcinoma that did not contain other common genetic alterations.¹⁶ TRKC fusion protein Tel-TRKC has been identified as the causative event in rare cancers such as secretory breast carcinoma (SBC),¹⁷ congenital fibrosarcoma (CFS),¹⁸ and congenital mesoblastic nephroma (CMN).¹⁹ In addition, there may be a role for small molecule inhibitors in

other cancer settings. For example, BDNF levels have been associated with unfavorable pathological parameters and adverse clinical outcome in breast cancer, and TRKB has been reported as a strong predictor of aggressive tumor growth in neuroblastoma.^{20–23} Selective TRK inhibitors, AZ623 and GNF-4256, have been shown to inhibit the growth of human neuroblastoma xenograft tumors and, in combination with chemotherapy, have prolonged inhibition of tumor regrowth.^{24,25} Moreover, high and increased expression of TRK receptors in pancreatic cancer correlates with tumor progression, perineural invasion, pain, and metastasis.^{7,26–28}

Given the growing evidence for a role of TRK in cancer there is interest in discovering developable selective TRK inhibitors for evaluation in the clinic. Here we describe the discovery of (R)-2-phenylpyrrolidine substituted imidazopyridazines as a novel class of selective pan-TRK inhibitors with efficacy in a KM12 rat tumor model.

The novel benzonitrile substituted imidazopyridazine **1** was identified as an inhibitor of TRKB (IC₅₀ = 83 nM) from screening using a TRKB biochemical inhibition assay (Scintillation Proximity Assay). Submicromolar cellular activity across the three TRK isoforms was shown in Ba/F3 assays where Ba/F3 cells were rendered TRKA, TRKB, and TRKC dependent and IL-3 independent by respectively overexpressing

Received: January 30, 2015

Accepted: March 16, 2015

Published: March 16, 2015

Table 1. Cellular Activities of Imidazopyridazines

compd	Cellular Ba/F3 assays ^a			WT ^b
	TRKA	TRKB	TRKC	
1	0.85	0.27	0.10	7.13
2	0.74	0.20	0.23	>10
3	0.050	0.021	0.006	3.92
4	0.17	0.12	0.075	1.01
5	0.076	0.027	0.040	1.92
6	0.006	0.007	0.003	3.00
7	0.027	0.013	0.004	2.53
8	0.52	0.13	0.020	5.89
9	0.17	0.050	0.011	>10
10	0.075	0.047	0.019	>10
11	0.068	0.029	0.008	>10
12	3.13	1.97	0.98	9.23
13	0.021	0.011	0.003	>10
14	0.003	0.001	0.001	>10
15	0.005	0.004	0.002	>10
16	0.001	0.001	<0.001	4.79
17	0.004	0.004	0.002	5.91

^aProliferation assays with Tel-TRK fusions; IC₅₀, μM. ^bProliferation assay using parental Ba/F3 cells.

the constitutively active Tel-TRKA, Tel-TRKB, and Tel-TRKC fusions (Table 1). In this assay setting, **1** showed differential cytotoxicity as compared to parental wild-type (WT) Ba/F3 cells grown in the presence of IL-3. The cellular kinase selectivity profile of **1** was determined in a Ba/F3 panel using Ba/F3 cells rendered IL-3 independent by stable transduction with 29 selected kinases activated by fusion with a dimerizing protein partner (e.g. BCR or Tel).²⁹ In this panel, **1** showed reasonable selectivity with submicromolar inhibitory activity for FLT3 and ROS (Scheme 1, Table 3).

The X-ray cocrystal structure of **1** showed binding to the inactivated (DFG-out) kinase domain of TRKC and forming a key hydrogen bond between N1 of the imidazopyridazine and the hinge amide NH of Met620 (Figure 1).^{30,31} The benzonitrile ring was wedged between phenyl rings from the gatekeeper Phe617, Phe698 from the DFG motif, and the phenyl ring of the benzylamino group of compound **1**. This

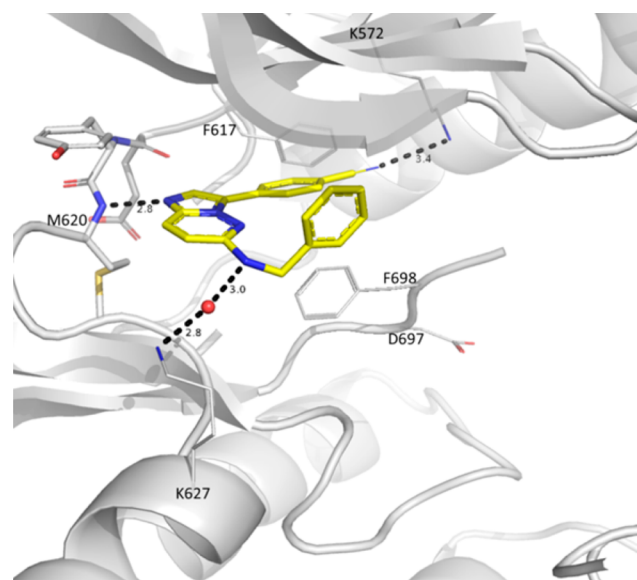


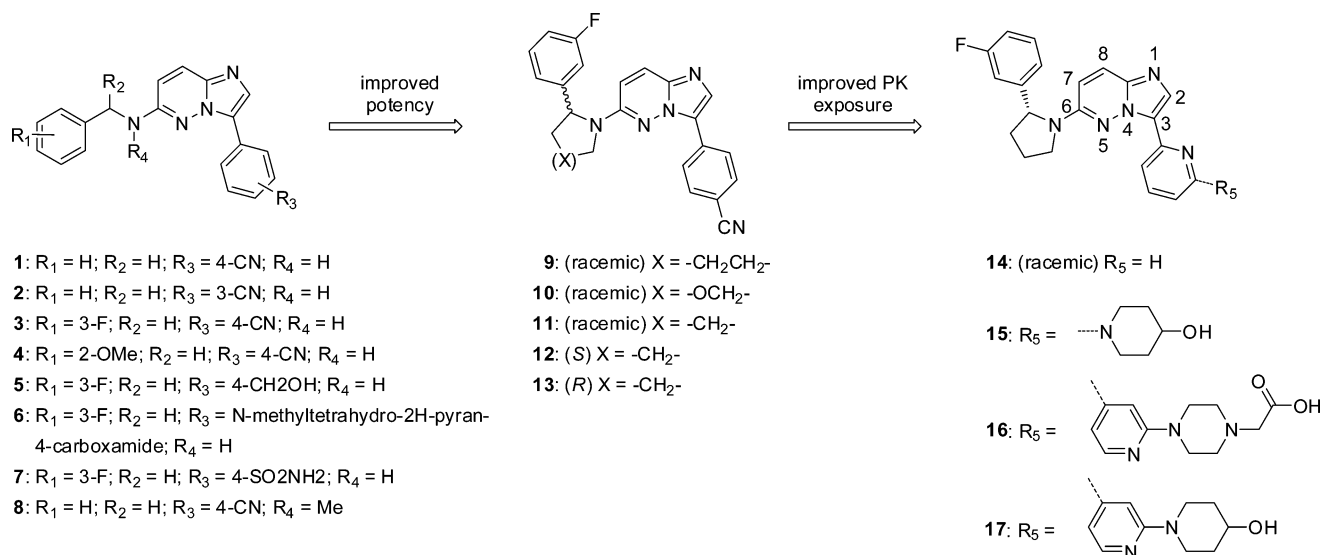
Figure 1. X-ray cocrystal structure of **1** (carbon in yellow) binding to the active site of TRKC kinase. Hydrogen bonds are depicted as dashed lines. Nitrogen atoms are shown in blue, oxygen atoms in red, and a water molecule depicted as a red sphere.

phenyl ring sits under the glycine-rich loop and faces the solvent exposed front of the binding pocket, lending itself to immediate structure–activity relationship (SAR) investigations.

Chemistry optimization was initiated with the goal of identifying compounds with improved potency and pharmacokinetic properties suitable for *in vivo* profiling. New compounds were screened for antiproliferative effects in Ba/F3-Tel-TRKA, TRKB, and TRKC assays, and cytotoxicity effects were compared with parental wild-type (WT) Ba/F3 cells. Initial efforts focused on exploring the SAR around the benzyl amine moiety (R₁, R₂, R₄) and the phenyl group linked to the imidazopyrimidine core (R₃) (Scheme 1 and Table 1).

From this work, it appeared that nitrile substitutions in the phenyl group (R₃) at the 3 or 4 ring-position were equally tolerated (**1** vs **2**). It was also observed that 3-substitution at the benzylamino phenyl ring (R₁) led to a 10-fold increase in

Scheme 1. Imidazopyridazines SAR Progression and Numbering Assignment



potency relative to the unsubstituted **1**, especially with EWG groups such as fluorine (**3** vs **4**). Shimming the phenyl ring (R_3) with the potency boosting 3-F substitution at R_1 furnished many tolerated functional groups that could either increase solubility or further drive potency such as hydroxymethyl derivative **5**, amide **6**, and sulfonamide **7**.

Methylation of the benzylic amine (R_4) led to no significant change in potency (**8** vs **1**) suggesting that the benzylic amine is not involved in a critical proton donating interaction.

Docking models using the cocrystal structure of **1** with TRKA supported that potency could be further increased by structurally rigidifying the benzyl amine moiety in a cyclic fashion by reducing conformational entropy. Cyclic piperidine, morpholine, and pyrrolidine analogues were synthesized as racemates (**9**, **10**, and **11**) and revealed a potency preference toward the five-membered heterocycle. A cocrystal structure between TRKA and **10** indicated a preference for the *R*-enantiomer and induced protein conformation change from the DFG-out to the DFG-in state, which allowed the fluorophenyl to bind near the ribose binding pocket (Figure 2).³⁰ Moreover,

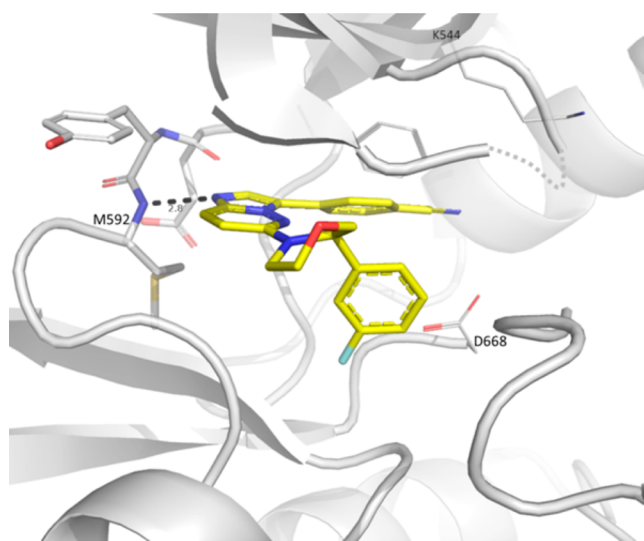


Figure 2. X-ray cocrystal structure of TRKA with **10**. The fluorophenyl points toward the pocket usually occupied by the ribose from ATP. The protein adopts a DFG-in conformation to allow for the fluorophenyl to bind. Although the **10** racemate was used for crystallization, only the *R*-enantiomer binds to TRKA. Color coding according to Figure 1.

the DFG-in conformation prevented a clash between Phe669 and the compound's fluorophenyl group. Chiral resolution of the pyrrolidine derivative **11** into its two enantiomers, **12** and **13**, indicated the *R*-enantiomer (**13**) as the more potent isomer, which also demonstrated a 2-fold activity improvement relative to acyclic compound **3**.

By maintaining the 3-F-phenylpyrrolidine in **11**, a subsequent round of optimization at R_3 was performed. This effort showed that replacing the 3-CN-phenyl moiety with a 2-pyridine (**14**) led to an 8–20-fold potency improvement across all three TRK isoforms.

The cocrystal structure of **14** with TRKA revealed an unanticipated flip of the compound around the imidazopyridazine core while maintaining the same key hinge interaction (Figure 3).³⁰ Binding could only be observed for the *R*-enantiomer where the 3-F-phenyl is optimally positioned in the

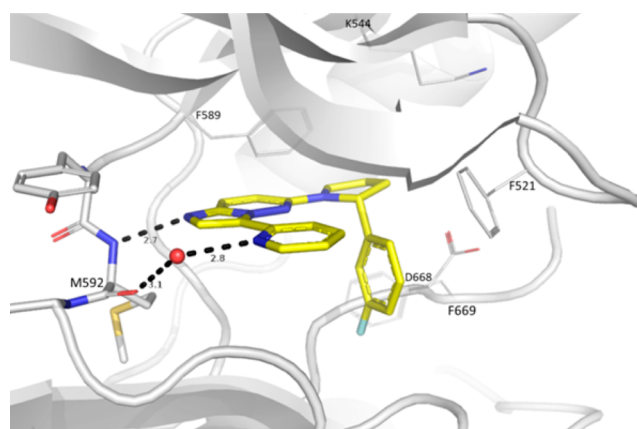


Figure 3. X-ray cocrystal structure of TRKA with the *R*-enantiomer of **14**. The protein adopts the DFG-in conformation. Compound **14** maintains the key hydrogen bond between the hinge NH of Met592 and N1 of imidazopyridazine. Surprisingly, the imidazopyridazine is now flipped. This allows for the fluorophenyl group to better fit the ribose binding pocket compared to **10**. Color coding according to Figure 1.

hydrophobic pocket originally occupied by Phe669 and provides excellent shape complementary, likely to contribute significantly to the observed potency improvement. Molecular modeling indicated that two distinct binding modes (i.e. core flipping) are indeed possible for the DFG-in conformation. The preferred binding mode probably depends upon the substitution on the 6-position of the imidazopyridazine. When this substitution is the (*R*)-phenylpyrrolidine, the “flipped” orientation appears to be preferred as the pyrrolidine anchors the phenyl group in the hydrophobic pocket.

It is worth noting that since our initial disclosure of the (*R*)-2-phenylpyrrolidine in 2008,³² this moiety has become a privileged TRK structure and was incorporated effectively in closely related scaffolds^{33–38} and on unrelated bicycle scaffolds.³⁹

The cocrystal structure of **14** indicated that the pyridine ring at the 3-position faces the solvent exposed front of the binding pocket, suggesting that polar groups in this area should be tolerated. Indeed, decorating the 3-position (R_5) of the pyridine maintained very good potency across the TRK isoforms (**15**, **16**, and **17**).

To determine the *in vivo* PK properties, **15**, **16**, and **17** were administered intravenously to Wistar or Sprague–Dawley rats. High plasma clearance (CL), moderate volume distribution (V_{ss}), and short half-life ($T_{1/2}$) were observed (Table 2). The plasma clearances of these compounds were about 82% (**16** and

Table 2. *In Vivo* Rat PK Properties after Dosing of 3 mg/kg IV and 10 mg/kg PO

rat PK ^a	15 ^b	16 ^b	17 ^c
CL (mL/min/kg)	56.9	45.5	45.2
V_{ss} (L/kg)	2.3	2.4	4.9
$T_{1/2}$ (h)	0.83	0.9	1.6
AUC PO (h·nM)	659	1897	1879
C_{max} PO (nM)	110	250	215
$F(\%)$ PO	10	26	27

^aRoute: Intravenous (3 mg/kg) and oral administrations (10 mg/kg). Formulation as a solution in 75% PEG300/25% D5W. ^bMale Sprague–Dawley rat. ^cMale Wistar rat.

17) and 100% (15) of rat hepatic blood flow (55 mL/min/kg). Compound 17, with an additional heterocyclic group between the pyridine and the solubilizing group, led to a higher volume of distribution (4.9 vs 2.3 L/kg), which resulted in a longer half-life (1.6 vs 0.9 h) compared to 15 and 16. When administered orally by gavage, 15 showed low bioavailability (10%), while 16 and 17 had 2.6-fold higher oral bioavailability (Table 2). In mouse brain tissue distribution studies, the AUC and C_{\max} ratios of brain to plasma were lower for 17 (~0.2) compared to 16 (~0.8) (Supporting Information).

Compounds 14, 16, and 17 were tested in the Ba/F3 panel and showed much improved selectivity across all the kinases when compared to 1 (Table 3; see Table 1 for TRK activity).

Table 3. Ba/F3 Cellular Kinase Panel (IC_{50} , μM)

Ba/F3 ^a	1	14	16	17
ABL ^b	3.8	NA	2.4	5.2
ALK ^c	4.8	6.3	1.2	3.0
ALK	3.1	NA	2.2	3.9
BRAF	2.5	NA	6.2	5.9
BMX	9.7	>10	2.7	4.3
FGFR3	3.9	9.5	4.9	5.0
FGFR4	5.9	9.2	5.3	4.4
FGR	6.4	8.7	2.8	5.9
FLT1	3.0	NA	2.6	5.3
FLT3	0.72	8.1	3.3	4.3
FMS	3.4	>10	2.5	5.3
IGF1R	4.0	NA	5.1	5.4
INSR	8.6	8.8	5.3	6.0
JAK2	4.7	6.7	2.7	5.6
KDR	4.1	6.5	1.0	5.0
KIT	2.2	5.5	0.79	7.0
LCK	2.0	NA	3.0	5.2
LYN	7.5	6.4	3.4	4.9
MER	5.4	NA	4.7	5.1
MET	5.1	7.7	4.3	5.7
PDGFR β	2.0	NA	2.2	4.6
RET	4.9	8.0	3.7	6.0
RON	6.1	NA	5.0	4.8
ROS	0.30	0.6	0.06	0.21
SRC	4.6	NA	2.5	4.6
SYK	4.0	NA	4.4	7.9
TIE1	5.5	6.5	4.3	5.5
TYRO3	NA	NA	5.2	5.0
ZAP70	6.4	NA	5.2	5.5

^aBa/F3 cells rendered IL-3 independent by stable transduction with the indicated kinase fused with a Tel dimerization partner unless otherwise specified. ^bBCR-ABL. ^cNMP-ALK.

The main kinase off-target activity remained ROS but with an improved selectivity index (SI) (SI < 3 for 1 and SI > 50 for 14, 16, and 17). This demonstrated that (R)-2-fluorophenylpyrrolidine-containing analogues were able to achieve higher potency as well as increased selectivity due to their high specificity at the hydrophobic pocket.

In addition, the anti-TRKA activity for compounds 16 and 17 was further demonstrated in two other cellular systems, Ba/F3 and KM12. In Ba/F3 cells engineered to express both TRKA and NGF, both compounds demonstrated potent antiproliferation activity with IC_{50} of 0.001 and 0.003 μM , respectively. In KM12 cells, derived from a colon cancer cell line that harbors the TPM3-TRKA fusion and is dependent on

TRKA kinase for proliferation and survival, the compounds were also very potent with IC_{50} of 0.001 and 0.01 μM , respectively.

By virtue of its pan-TRK *in vitro* potency, good selectivity, relatively low brain exposure, and overall acceptable PK properties, 17 (GNF-8625) was selected for *in vivo* efficacy studies (synthesis in Supporting Information). In a tumor xenograft model derived from the KM12 cell line,⁴⁰ 17 demonstrated *in vivo* antitumor efficacy when administered at ascending doses twice daily (bid) for 14 days in rats (Figure 4).

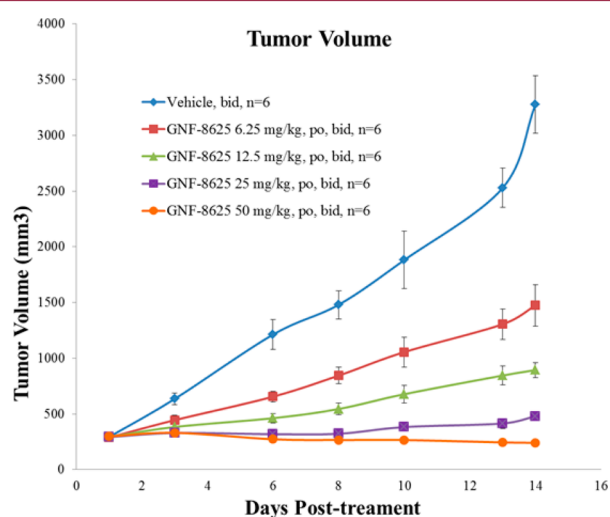


Figure 4. KM12 efficacy model in female CRL RNU nude rats with compound 17 (GNF-8625). Animals were transplanted with KM12 tumor tissues, and dosing began 10 days postimplant. Vehicle and 17 were dosed twice a day (bid) for 14 days. Efficacy measured as tumor volume.

In this study, 17 induced 20% tumor regression at 50 mg/kg bid and achieved partial tumor growth inhibition at 6.25, 12.5, and 25 mg/kg bid, in a dose-dependent manner. A dose proportional increase in exposure of compound 17 was observed, and at the highest doses, a slight increase in body weight was observed (Supporting Information).

In summary, using a TRK/ligand cocrystal structural guided approach, we have developed a series of potent, selective, and efficacious (R)-2-phenylpyrrolidine substituted imidazopyridazine TRK inhibitors. This work has unveiled the (R)-2-phenylpyrrolidine as a privileged moiety for TRK inhibitors due to its optimal shape complementarity to the TRK protein's hydrophobic pocket available in the "DFG-in" conformation.

■ ASSOCIATED CONTENT

📄 Supporting Information

Experimental procedures, characterization of compounds, kinase selectivity, ADMET data for compound 17, and details of *in vitro* and *in vivo* assays. This material is available free of charge via the Internet at <http://pubs.acs.org>.

■ AUTHOR INFORMATION

✉ Corresponding Author

*Tel: 858-332-4736. E-mail: vmolteni@gnf.org.

📍 Present Addresses

[†]Novartis Pharma AG, Novartis Institutes for Biomed. Research, Postfach, CH-4002 Basel, Switzerland.

[‡]Loma Linda University Medical Center, Rehabilitation Institute, 25333 Barton Road, Loma Linda, California 92354, United States.

[§]Sanofi Oncology, 640 Memorial Drive, Cambridge, Massachusetts 02139, United States.

^{||}Parallel Computing Laboratories, Inc., 3525 Del Mar Heights Road, #288, San Diego, California 92130, United States.

[†]Novartis Institutes for BioMedical Research, Inc. 250 Massachusetts Avenue, Cambridge, Massachusetts 02139, United States.

[#]Novartis Pharmaceuticals Corporation, One Health Plaza, East Hanover, New Jersey 07936, United States.

Author Contributions

All authors have given approval to the final version of the manuscript.

Notes

The authors declare no competing financial interest.

ACKNOWLEDGMENTS

We thank Daniel Raymond and Thomas H. Marsilje for help in proof reading.

ABBREVIATIONS

TRK, tropomyosin receptor kinase; NGF, nerve growth factor; BDNF, brain-derived neurotrophic factor

REFERENCES

- (1) Huang, E. J.; Reichardt, L. F. TRK Receptors: Roles in Neuronal Signal Transduction. *Annu. Rev. Biochem.* **2003**, *72*, 609–642.
- (2) Pierotti, M. A.; Greco, A. Oncogenic Rearrangements of the NTRK1/NGF Receptor. *Cancer. Lett.* **2006**, *232*, 90–98.
- (3) Lei, L.; Parada, L. F. Transcriptional Regulation of TRK Family Neurotrophin Receptors. *Cell. Mol. Life Sci.* **2007**, *64*, 522–532.
- (4) Lagadec, C.; Meignan, S.; Adriaenssens, E.; Foveau, B.; Vanhecke, E.; Romon, R.; Toillon, R. A.; Oxombre, B.; Hondermarck, H.; Le Bourhis, X. TRKA Overexpression Enhances Growth and Metastasis of Breast Cancer Cells. *Oncogene* **2009**, *28*, 1960–1970.
- (5) Borrello, M. G.; Bongarzone, I.; Pierotti, M. A.; Luksch, R.; Gasparini, M.; Collini, P.; Pilotti, S.; Rizzetti, M. G.; Mondellini, P.; De Bernardi, B.; Di Martino, D.; Garaventa, A.; Brisigotti, M.; Tonini, G. P. TRK and ret Proto-Oncogene Expression in Human Neuroblastoma Specimens: High Frequency of TRK Expression in Non-Advanced Stages. *Int. J. Cancer* **1993**, *54*, 540–545.
- (6) Ma, J.; Jiang, Y.; Jiang, Y.; Sun, Y.; Zhao, X. Expression of Nerve Growth Factor and Tyrosine Kinase Receptor A and Correlation with Perineural Invasion in Pancreatic Cancer. *J. Gastroenterol. Hepatol.* **2008**, *23*, 1852–1859.
- (7) Zhu, Z.; Friess, H.; diMola, F. F.; Zimmermann, A.; Graber, H. U.; Korc, M.; Buchler, M. W. Nerve Growth Factor Expression Correlates with Perineural Invasion and Pain in Human Pancreatic Cancer. *J. Clin. Oncol.* **1999**, *17*, 2419–2428.
- (8) Festuccia, C.; Muzi, P.; Gravina, G. L.; Millimaggi, D.; Specia, S.; Dolo, V.; Ricevuto, E.; Vicentini, C.; Bologna, M. Tyrosine Kinase Inhibitor CEP-701 Blocks the NTRK1/NGF Receptor and Limits the Invasive Capability of Prostate Cancer Cells in vitro. *Int. J. Oncol.* **2007**, *30*, 193–200.
- (9) Davidson, B.; Reich, R.; Lazarovici, P.; Nesland, J. M.; Skrede, M.; Risberg, B.; Trope, C. G.; Florenes, V. A. Expression and Activation of the Nerve Growth Factor Receptor TRKA in Serous Ovarian Carcinoma. *Clin. Cancer. Res.* **2003**, *9*, 2248–2259.
- (10) Martin-Zanca, D.; Hughes, S. H.; Barbacid, M. A Human Oncogene Formed by the Fusion of Truncated Tropomyosin and Protein Tyrosine Kinase Sequences. *Nature* **1986**, *319*, 743–748.
- (11) Butti, M. G.; Bongarzone, I.; Ferraresi, G.; Mondellini, P.; Borrello, M. G.; Pierotti, M. A. A Sequence Analysis of the Genomic Regions Involved in the Rearrangements Between TPM3 and NTRK1

Genes Producing TRK Oncogenes in Papillary Thyroid Carcinomas. *Genomics* **1995**, *28*, 15–24.

(12) Greco, A.; Mariani, C.; Miranda, C.; Pagliardini, S.; Pierotti, M. A. Characterization of the NTRK1 Genomic Region Involved in Chromosomal Rearrangements Generating TRK Oncogenes. *Genomics* **1993**, *18*, 397–400.

(13) Bounacer, A.; Schlumberger, M.; Wicker, R.; Du-Villard, J. A.; Caillou, B.; Sarasin, A.; Suarez, H. G. Search for NTRK1 Proto-Oncogene Rearrangements in Human Thyroid Tumours Originated After Therapeutic Radiation. *Br. J. Cancer* **2000**, *82*, 308–314.

(14) Beimfohr, C.; Klugbauer, S.; Demidchik, E. P.; Lengfelder, E.; Rabes, H. M. NTRK1 Re-Arrangement In Papillary Thyroid Carcinomas of Children After the Chernobyl Reactor Accident. *Int. J. Cancer* **1999**, *80*, 842–847.

(15) Alberti, L.; Carniti, C.; Miranda, C.; Roccatto, E.; Pierotti, M. A. RET and NTRK1 Proto-Oncogenes in Human Diseases. *J. Cell. Physiol.* **2003**, *195*, 168–186.

(16) Vaishnavi, A.; Capelletti, M.; Le, A. T.; Kako, S.; Butaney, M.; Ercan, D.; Mahale, S.; Davies, K. D.; Aisner, D. L.; Pilling, A. B.; Berge, E. B.; Kim, J.; Sasaki, H.; Park, S.; Kryukov, G.; Garraway, L. A.; Hammerman, P. S.; Haas, J.; Andrews, S. W.; Lipson, D.; Stephens, P. J.; Miller, V. A.; Varella-Garcia, M.; Jänne, P. A.; Doebele, R. C. Oncogenic and Drug-Sensitive NTRK1 Rearrangements in Lung Cancer. *Nat. Med.* **2013**, *19*, 1469–1472.

(17) Tognon, C.; Knezevich, S. R.; Huntsman, D.; Roskelley, C. D.; Melnyk, N.; Mathers, J. A.; Becker, L.; Carneiro, F.; MacPherson, N.; Horsman, D.; Poremba, C.; Sorensen, P. H. B. Expression of the ETV6-NTRK3 Gene Fusion as a Primary Event in Human Secretory Breast Carcinoma. *Cancer Cell* **2002**, *2*, 367–376.

(18) Lannon, C. L.; Sorensen, P. H. B. ETV6-NTRK3: a Chimeric Protein Tyrosine Kinase with Transformation Activity in Multiple Cell Lineages. *Semin. Cancer Biol.* **2005**, *15*, 215–223.

(19) Watanabe, N.; Kobayashi, H.; Hirama, T.; Kikuta, A.; Koizumi, S.; Tsuru, T.; Kaneko, Y. Cryptic t(12;15)(p13;q26) Producing the ETV6-NTRK3 Fusion Gene and No Loss of IGF2 Imprinting in Congenital Mesoblastic Nephroma with Trisomy 11 Fluorescence in situ Hybridization and IGF2 Allelic Expression Analysis. *Cancer Genet. Cytogenet.* **2002**, *136*, 10–16.

(20) Patani, N.; Jiang, W. G.; Mokbel, K. Brain derived Neurotrophic Factor Expression Predicts Adverse Pathological and Clinical Outcomes in Human Breast Cancer. *Cancer Cell. Int.* **2011**, *11*, 23–30.

(21) Roesler, R.; Brunetto de Farias, C.; Abujamra, A. L.; Brunetto, A. L.; Schwartzmann, G. BDNF/TrkB Signaling as an Anti-Tumor Target. *Expert Rev. Anticancer Ther.* **2011**, *11*, 1473–1475.

(22) Izbicka, E.; Izbicki, T. Therapeutic Strategies for the Treatment of Neuroblastoma. *Curr. Opin. Investig. Drugs* **2005**, *6*, 1200–1214.

(23) Douma, S.; Van Laar, T.; Zevenhoven, J.; Meuwissen, R.; Van Garderen, E.; Peeper, D. S. Suppression of Anoikis and Induction of Metastasis by the Neurotrophic Receptor TRKB. *Nature* **2004**, *430*, 1034–1039.

(24) Zage, P. E.; Graham, T. C.; Zeng, L.; Fang, W.; Pien, C.; Thress, K.; Omer, C.; Brown, J. L.; Zweidler-McKay, P. A. The Selective Trk Inhibitor AZ623 Inhibits Brain-Derived Neurotrophic Factor-Mediated Neuroblastoma Cell Proliferation and Signaling and is Synergistic with Topotecan. *Cancer* **2011**, *117*, 1321–1329.

(25) Croucher, J. L.; Iyer, R.; Li, N.; Molteni, V.; Loren, J.; Gordon, W. P.; Tuntland, T.; Liu, B.; Brodeur, G. M. TrkB Inhibition by GNF-4256 Slows Growth and Enhances Chemotherapeutic Efficacy in Neuroblastoma Xenografts. *Cancer Chemother. Pharmacol.* **2015**, *75*, 131–41.

(26) Miknyoczki, S. J.; Chang, H.; Klein-Szanto, A.; Dionne, C. A.; Ruggeri, B. A. The TRK Tyrosine Kinase Inhibitor CEP-701 (KT-5555) Exhibits Significant Antitumor Efficacy in Preclinical Xenograft Models of Human Pancreatic Ductal Adenocarcinoma. *Clin. Cancer Res.* **1999**, *5*, 2205–2212.

(27) Ketterer, K.; Rao, S.; Friess, H.; Weiss, J.; Buechler, M. W.; Korc, M. Reverse Transcription-PCR Analysis of Laser-Captured Cells Points to Potential Paracrine and Autocrine Actions of Neurotrophins in Pancreatic Cancer. *Clin. Cancer Res.* **2003**, *9*, 5127–5136.

(28) Sclabas, G. M.; Fujioka, S.; Schmidt, C.; Li, Z.; Frederick, W. A. I.; Yang, W.; Yokoi, K.; Evans, D. B.; Abbruzzese, J. L.; Hess, K. R.; Zhang, W.; Fidler, I. J.; Chiao, P. Overexpression of Tropomyosin-Related Kinase B in Metastatic Human Pancreatic Cancer Cells. *Clin. Cancer Res.* **2005**, *11*, 440–449.

(29) Melnick, J. S.; Janes, J.; Kim, S.; Chang, J. Y.; Sipes, D. G.; Gunderson, D.; James, L.; Matzen, J. T.; Garcia, M. E.; Hood, T. L.; Beigi, R.; Xia, G.; Harig, R. A.; Asatryan, H.; Yan, S. F.; Zhou, Y.; Gu, X. J.; Saadat, A.; Zhou, V.; King, F. J.; Shaw, C. M.; Su, A. I.; Downs, R.; Gray, N. S.; Schultz, P. G.; Warmuth, M.; Caldwell, J. S. An Efficient Rapid System for Profiling the Cellular Activities of Molecular Libraries. *Proc. Natl. Acad. Sci. U.S.A.* **2006**, *103*, 3153–3158.

(30) Structure coordinates have been deposited into the PDB: 4YMJ; 4YNE; 4YPS.

(31) Zuccotto, F.; Ardini, E.; Casale, E.; Angiolini, M. Through the “Gatekeeper Door”: Exploiting the Active Kinase Conformation. *J. Med. Chem.* **2010**, *53*, 2681–2694.

(32) Ferrand, S.; Glickman, F.; Leblanc, C.; Ritchie, C.; Shaw, D.; Stiefl, N. J.; Furet, P.; Imbach, P.; Stauffer, F.; Capraro, H. G.; Gessier, F.; Gaul, C.; Albaugh, P.; Chopiuk, G. Heterocyclic Compounds as Antiinflammatory Agents. WO/2008/052734; International Application No. PCT/EP2007/009382; May 8, 2008.

(33) Andrews, S. W.; Haas, J.; Jiang, Y.; Zhang, G. Substituted Imidazo[1,2b]pyridazine Compounds as TRK Kinase Inhibitors. WO/2010/033941; International Application No. PCT/US2009/057729; March 25, 2010.

(34) Haas, J.; Andrews, S. W.; Jiang, Y.; Zhang, G. Substituted Pyrazolo[1,5-a]pyrimidine Compounds as TRK Kinase Inhibitors. WO/2010/048314 A1; International Application No. PCT/US2009/061519; April 29, 2010.

(35) Allen, S.; Andrews, S. S.; Condroski, K. R.; Haas, J.; Huang, L.; Jiang, Y.; Kercher, T.; Seo, J. Substituted Pyrazolo[1,5-a]pyrimidine Compounds as TRK Kinase Inhibitors. WO/2011/006074 A1; International Application No. PCT/US2010/041538; January 11, 2011.

(36) Andrews, S. W.; Condroski, K. R.; Haas, J.; Jiang, Y.; Kolakowski, G. R.; Seo, J.; Yang, H. W.; Zhao, Q. Macrocyclic Compounds as Trk Kinase Inhibitors. WO/2011/146336 A1; International Application No. PCT/US2011/036452; November 24, 2011.

(37) Sasmal, P. K.; Ahmed, S.; Tehim, A.; Pradkar, V.; Dattatreya, P. M.; Mavinahalli, N. J. Substituted Pyrazolo[1,5-a]pyridine as Tropomyosin Receptor Kinase (Trk) Inhibitors. WO/2013/088256 A1; International Application No. PCT/IB2012/003012; June 20, 2013.

(38) Sasmal, P. K.; Ahmed, S.; Prabhu, G.; Tehim, A.; Pradkar, V.; Dattatreya, M. P.; Mavinahalli, N. J. Substituted Heterocyclic Compounds as Tropomyosin Receptor Kinase A (TRKA) Inhibitors. WO/2013/088257 A1; International Application No. PCT/IB2012/003022; June 20, 2013.

(39) Stachel, S. J.; Sanders, J. M.; Henze, D. A.; Rudd, M. T.; Su, H. P.; Li, Y.; Nanda, K. K.; Egbertson, M. S.; Manley, P. J.; Jones, K. L. G.; Brnardic, E. J.; Green, A.; Grobler, J. A.; Hanney, B.; Leidl, M.; Lai, M. T.; Munshi, V.; Murphy, D.; Rickert, K.; Riley, D.; Krasowska-Zoladek, A.; Daley, C.; Zuck, P.; Kane, S. A.; Bilodeau, M. T. Maximizing Diversity from a Kinase Screen: Identification of Novel and Selective pan-Trk Inhibitors for Chronic Pain. *J. Med. Chem.* **2014**, *57*, 5800–5816.

(40) Unpublished data.